

# Unidirectional light emission from high- $Q$ modes in optical microcavities due to resonance-enhanced dynamical tunneling

Jan Wiersig

*Institut für Theoretische Physik, Universität Bremen, Postfach 330 440, D-28334 Bremen, Germany\**

Martina Hentschel

*Institut für Theoretische Physik, Universität Regensburg, D-93040 Regensburg, Germany and  
ATR Wave Engineering Laboratories, 2-2-2 Hikaridai, Seika-cho, Soraku-gun, Kyoto 619-0228, Japan*

(Dated: December 21, 2018)

We introduce a new scheme to design optical microcavities supporting high- $Q$  modes with unidirectional light emission. This is achieved by coupling a low- $Q$  mode with unidirectional emission to a high- $Q$  mode without directed emission. The coupling is due to enhanced dynamical tunneling near an avoided resonance crossing. Numerical results for a microdisk with a suitably positioned air hole demonstrate the feasibility and the potential of this concept.

PACS numbers: 42.55.Sa, 42.25.-p, 42.60.Da, 05.45.Mt

Confinement of light in dielectric microcavities is important for a wide range of research areas and applications, such as, e.g., cavity quantum electrodynamics and novel light sources [1]. A key quantity characterizing a resonant optical mode of a cavity is its quality factor  $Q = \omega/\Delta\omega$ , where  $\omega$  is the mode frequency and  $\Delta\omega$  is the linewidth. A large  $Q$ -factor is a basic requirement for low threshold lasing, high sensor sensitivity, narrow wavelength-selective filtering, and strong light-matter interaction. Whispering-gallery modes (WGMs) in microdisks [2], microspheres [3], and microtori [4] have *ultra-high*  $Q$ -factors. For state-of-the-art semiconductor microdisks, the record  $Q$ -factor is  $> 3.5 \times 10^5$  [5, 6].

The applicability of such cavities as microlasers and single-photon sources, however, is limited by the isotropy of light emission. The best directionality so far is provided by VCSEL-micropillars; see, e.g., Ref. [7]. The emission is *unidirectional* at the cost of a reduced  $Q$ -factor, typically well below 10 000. With present technology, there is a trade-off between  $Q$ -factor and directionality.

This dilemma remains when breaking the rotational symmetry of a microdisk. Shape deformation [8, 9] allows improved directionality of emission due to *refractive escape*, but the  $Q$ -factors are significantly spoiled. Unidirectional emission has been reported for rounded triangles [10] with  $Q \approx 35$  and for spiral-shaped disks [11]. In the latter case, a strong degradation of the cavity  $Q$  allows lasing operation only for spirals of the size of conventional edge emitting lasers.

Another approach is to break the symmetry with the objective to modify the evanescent leakage (the optical analogue of tunneling) from WGMs, thereby keeping the high  $Q$ -factor. Unidirectional lasing from a double-disk structure consisting of a bottom high- $Q$  disk and a top low- $Q$  disk with an opening has been reported in Ref. [12]. Unfortunately, the study was restricted to the near-field pattern. Another suggestion has been to introduce a linear defect structure into the evanescent inner region of WGMs [13]. Emission into four directions

from nearly spherical fused-silica cavities with ultra-high  $Q$ -factors has been reported in Ref. [14]. This surprising phenomenon had been explained with *dynamical tunneling* from a WGM to the exterior of the cavity. Dynamical tunneling is a generalization of conventional tunneling which allows to pass not only through an energy barrier but also through other kinds of dynamical barriers in phase space [15].

In this Letter, we propose to overcome the trade-off between  $Q$ -factor and directionality by combining dynamical tunneling and refractive escape. We couple a high- $Q$  mode and a low- $Q$  mode (LQM) with strong emission directionality using *enhanced dynamical tunneling near avoided resonance crossings* (ARCs). When varying an external parameter, two types of ARCs are possible in complex frequency space  $\omega - i\Delta\omega/2$  [16]. The strong coupling situation exhibits a frequency repulsion and a linewidth crossing. By varying the external parameter through a frequency repulsion the eigenstates interchange their identity. Correspondingly, the spatial mode characteristics such as, e.g., the far-field patterns switch their identity. The weak coupling situation consists of a frequency crossing and a linewidth repulsion. In such a case the eigenstates, and also the spatial mode characteristics, do not interchange but only intermix near the crossing point, and the high  $Q$ -factor is essentially maintained. We exploit this "hybridization" effect by varying an external parameter to tune the frequencies such that an ARC occurs between a high- $Q$  mode and a LQM with strong emission directionality. Even for weak intermixing, the dominant contribution to the far-field pattern comes from the LQM. This scheme allows the systematic design of modes with high  $Q$ -factors and highly directed far-field patterns.

We demonstrate the applicability of this scheme by a theoretical study of a semiconductor microdisk with a circular-shaped air hole as illustrated in Fig. 1. Different versions of such an annular cavity have been studied in the context of quantum chaos [17], optomechanical probes of resonances [18] and dynamical tunneling [19]. The closed system with perfectly reflecting walls, the annular billiard, has been used as model for dynamical tunneling [20, 21].

---

\*Electronic address: jwiersig@itp.uni-bremen.de

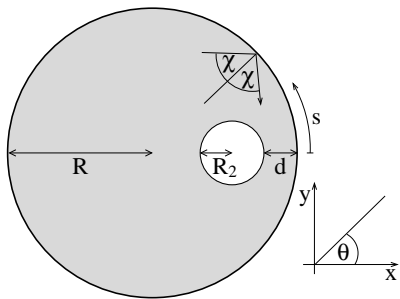


FIG. 1: Schematic top view of the annular cavity with radius  $R$ . The radius of the air hole is  $R_2$ , the minimal distance to the circumference of the disk is  $d$ . The direction of the outgoing light is characterized by the angle  $\theta$ .

Holes with radii  $\geq 100\text{nm}$  can be pierced through the disk surface by techniques currently applied to photonic crystal membrane cavities, see, e.g., Ref. [22]. In Ref. [23] square-shaped holes had been introduced into a large GaAs microdisk to reduce the laser threshold by perturbing the nonlasing modes. Our model calculations apply to a small GaAs microdisk of radius  $R = 1\mu\text{m}$ . Similar kinds of disks have been used recently to demonstrate strong coupling between excitons and photons for a single quantum dot [24]. We choose a slab thickness of  $375\text{nm}$ , a temperature of  $4\text{K}$  and a free-space wavelength  $\lambda$  close to  $900\text{nm}$ . This results in an effective index of refraction  $n_{\text{eff}} = 3.3$  for the transverse magnetic polarization with the electric field perpendicular to the disk plane. Although we focus on transverse magnetic polarization, the conclusions are the same for transverse electric polarization.

We use the boundary element method [25] and the  $S$ -matrix approach [17] to compute the spatial profile of the electromagnetic field, the  $Q$ -factors and the normalized frequencies  $\Omega = \omega R/c$ ,  $c$  being the speed of light in vacuum. According to the discrete symmetry, the modes are divided into even and odd symmetry classes.

A WGM in a disk without hole is characterized by azimuthal and radial mode numbers  $(m, n)$ . Clearly, the introduction of a hole modifies a  $\text{WGM}_{m,n}$  with large  $n$  strongly. As can be seen from the example in Fig. 2(a) such modes can have directed emission due to refractive escape. However, the  $Q$ -factors of these modes are low. In contrast, a  $\text{WGM}_{m,n}$  with small  $n$  is nearly unaffected, see Fig. 2(b). Such modes have high  $Q$  factors and are expected to emit without any preferred direction [13]. Here, we encounter the trade-off between  $Q$ -factors and directionality in a single cavity.

As external parameter we use the minimal distance  $d$  of the hole to the circumference of the disk. Figure 3(a) shows the normalized frequencies of all even-symmetry modes in the interval  $[6.97, 7.05]$  corresponding to  $\lambda$  close to  $900\text{nm}$ . This interval shows the typical scenario. For  $d/R > 0.35$ , WGMs such as  $\text{WGM}_{19,1}$  (solid line) and  $\text{WGM}_{15,2}$  (dotted) are much less affected by moving the hole than LQMs (dashed). With decreasing  $d/R$  all frequencies blueshift since dielectric material is effectively removed from the WGM region. This results in ARCs between WGMs and LQMs, see Figs. 3(a) and (b). At  $d/R \approx 0.24$  a frequency repulsion

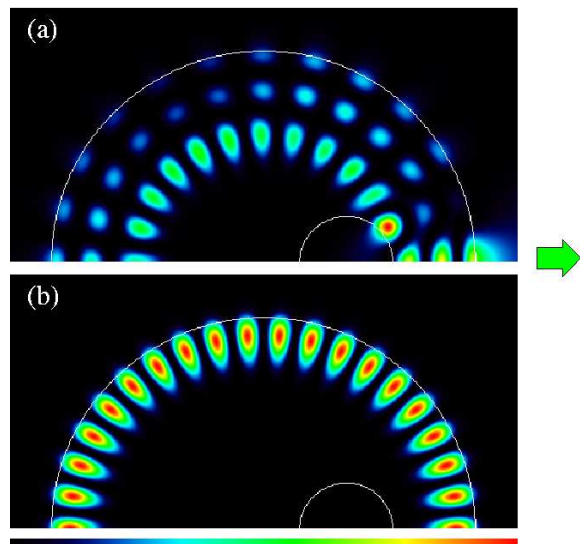


FIG. 2: (Color online) (a) Calculated near-field intensity pattern for LQM,  $\Omega = 7.0599$ ,  $Q \approx 300$ , even symmetry,  $R_2/R = 0.22$  and  $d/R = 0.389$ . The arrow shows the direction of light emission. (b)  $\text{WGM}_{19,1}$ ,  $\Omega = 7.0278$ ,  $Q \approx 553000$ .

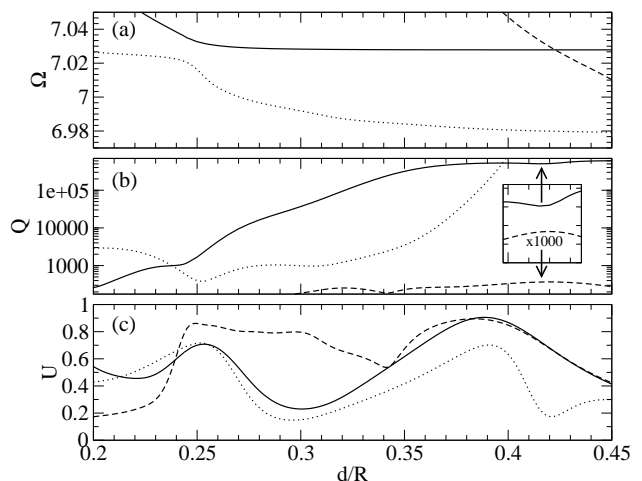


FIG. 3: Normalized frequencies (a) and  $Q$ -factors (b) of even-symmetry modes versus parameter  $d$  at fixed  $R_2/R = 0.22$ . Inset, magnification of the linewidth repulsion at  $d/R \approx 0.423$  in linear scale. For clarity, the low- $Q$  branch has been multiplied by a factor of 1000. (c) Fraction  $U$  of emitted light into  $|\theta| \leq 40^\circ$  for the same modes as in (a) and (b).

together with a linewidth ( $Q$ -factor) crossing takes place. At  $d/R \approx 0.423$  we observe a frequency crossing and a linewidth repulsion; cf. inset.

Figure 3(c) shows the directionality  $U$  versus  $d$ . We define  $U$  as the fraction of light radiation into an angular range of  $\pm 40^\circ$  around  $\theta = 0^\circ$ . Remarkably, near the frequency crossing at  $d/R \approx 0.423$  the directionality of  $\text{WGM}_{19,1}$  and of the LQM behave in exactly the same way. Gradually decreasing  $d/R$ , the directionality of the WGM remains close to that of the LQM until it reaches the maximum at  $d/R \approx 0.389$ ,

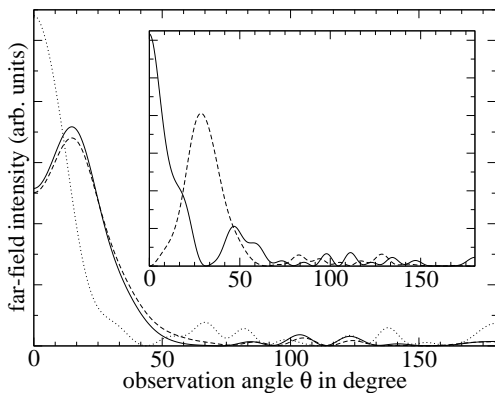


FIG. 4: Angular dependence of the far-field intensity pattern for WGM<sub>19,1</sub> (solid line) and LQM (dashed) both having even symmetry for  $R_2/R = 0.22$  and  $d/R = 0.389$ ; cf. Fig. 2. Dotted line belongs to WGM<sub>34,1</sub>,  $\Omega = 11.8833$ . Inset, even (solid) and odd (dashed) symmetry of WGM<sub>36,1</sub>,  $d/R = 0.4478$ ,  $\Omega = 12.5241$ .

where 90% of the light is emitted into a range of  $\pm 40^\circ$ . Figure 4 shows that at this value of  $d$  the angular emission pattern of the WGM and the LQM are almost identical. The far-field pattern has a narrow beam divergence angle of about  $57^\circ$  (full width at half maximum). The spectacular finding is that a WGM with ultra-high  $Q \approx 553000$  has highly-directed emission. This is explained by the hybridization of modes near the ARC. Note that even a small contribution of the LQM to the WGM dominates the far-field pattern, because of the strong leakiness of the LQM.

Two additional features in Fig. 3(c) fit naturally into this scheme. First, the directionality of the remaining WGM<sub>15,2</sub> resembles the one of the LQM not to such a high degree as in the case before since the frequency mismatch is larger. Second, the local maximum of the directionality at  $d/R \approx 0.254$  of both WGMs is located near the ARC of both modes.

To see the relation to dynamical tunneling we have to compare mode patterns with ray dynamics. A common approach in the field of quantum chaos is to superimpose the Husimi function (smoothed Wigner function) of a mode onto the Poincaré section [26] as shown in Fig. 5. The Poincaré section restricts the phase space of rays to the outer boundary of the cavity. The remaining variables are  $(s, \sin \chi)$  where  $s$  is the arclength along the circumference of the disk and  $\chi$  is the angle of incidence measured from the surface normal; cf. Fig. 1. A good visualisation of the dynamics is achieved by reflecting the rays a finite number of times in the closed cavity with perfectly reflecting outer boundary [17]. The phase space of the annular cavity contains two regular regions defined by  $|\sin \chi| > 1 - d/R$ . A ray with such a large angle of incidence never encounters the hole. It rotates as whispering-gallery trajectory clockwise,  $\sin \chi > 0$ , or counterclockwise,  $\sin \chi < 0$ . In the Poincaré section the ray is confined to a line  $\sin \chi = \text{const}$ . In particular, it cannot enter the region  $|\sin \chi| < 1 - d/R$ . For small  $R_2/R$ , this region is dominated by chaotic trajectories hitting the hole several times and thereby filling this phase space area in a pseudo-random fashion. Embedded into the chaotic region is the leaky region

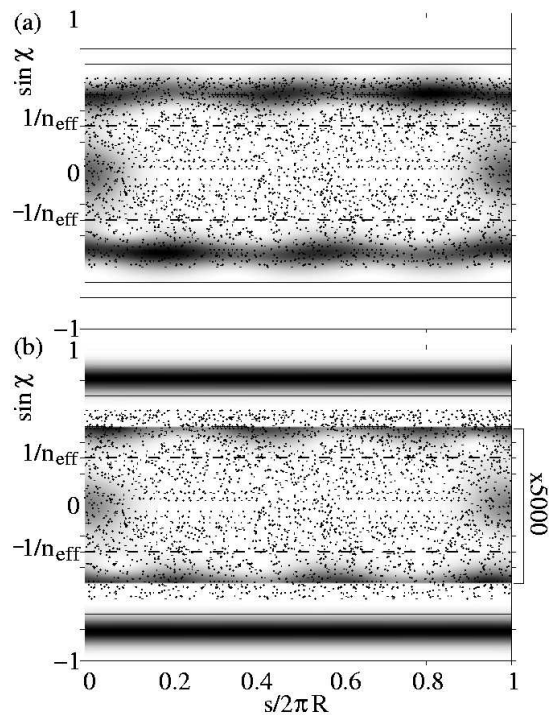


FIG. 5: Poincaré section (dots and solid lines) and Husimi function (shaded regions) of modes in Fig. 2. (a) LQM. (b) WGM<sub>19,1</sub>, the intensity inside the region  $|\sin \chi| \leq 1/2$  is multiplied by a factor of 5000 to allow for a comparison with the LQM. The dashed lines mark the leaky region  $[-1/n_{\text{eff}}, 1/n_{\text{eff}}]$ .

$|\sin \chi| < 1/n_{\text{eff}}$ . In the open cavity, a ray entering this region escapes refractively according to Snell's and Fresnel's laws.

The Husimi function of the LQM is restricted to the chaotic part of phase space, see Fig. 5(a). The significant overlap with the leaky region explains the low  $Q$ -factor. In contrast, the WGM lives mainly in the regular region around  $\sin \chi = m/n_{\text{eff}}\Omega \approx 0.82$ , see Fig. 5(b), far away from the leaky region ensuring a high  $Q$ -factor. However, a small contribution tunnels from the regular to the chaotic region. To highlight this contribution, the intensity inside the region  $|\sin \chi| \leq 1/2$  is multiplied by a factor of 5000. The striking similarity to the LQM in Fig. 5(a) carries over to their far-field patterns in Fig. 4.

Figure 6(a) shows the directionality in various regions of the normalized frequency  $\Omega$ . These examples illustrate that for lower (higher) frequency less (more) peaks appear. This is fully consistent with the fact that the larger the frequency the higher is the density of modes and therefore the larger the number of ARCs.

The best emission directionality has been found for the WGM<sub>34,1</sub> with normalized frequency  $\Omega \approx 11.88$ , which corresponds to  $R = 1.7\mu\text{m}$  at  $\lambda \approx 900\text{nm}$  or  $R = 1\mu\text{m}$  at  $\lambda \approx 530\text{nm}$ . The maximum in  $U$  is at  $d/R = 0.399$ , see Fig. 6(a). The far-field pattern is shown in Fig. 4 as dotted line. The emission is unidirectional with an angular divergence of  $28^\circ$  which is much smaller than the values reported for rounded triangles ( $90^\circ$ ) [10] and spiral-shaped disks ( $60^\circ$ ) [11], and

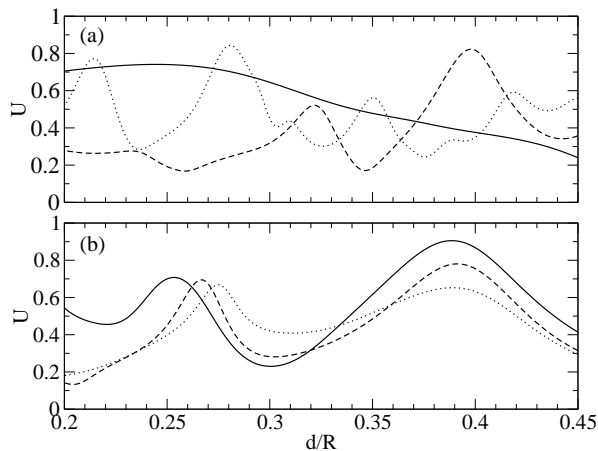


FIG. 6: (a) Directionality vs.  $d$  for various frequencies  $\Omega$  at fixed  $R_2/R = 0.22$ .  $\text{WGM}_{15,1}$  with  $\Omega \approx 5.71$  (solid line),  $\text{WGM}_{34,1}$  with  $\Omega \approx 11.88$  (dashed),  $\text{WGM}_{38,1}$  with  $\Omega \approx 13.16$  (dotted). (b)  $\text{WGM}_{19,1}$  for various hole radii.  $R_2/R = 0.22$  (solid),  $R_2/R = 0.28$  (dashed), and  $R_2/R = 0.315$  (dotted).

only 50% larger than that of a VCSEL-micropillar of the same radius [7]. The  $Q$ -factor is in this case so huge that our numerics is pushed to the limit; as a conservative lower bound we estimate  $Q \approx 10^8$ . In praxis, the  $Q$ -factor will be limited by absorption [2] and surfaces roughness [27]. Further numerical data (not shown) indicates that the unidirectional emission persists in the presence of surface roughness.

The directionality for different values of the hole radius,  $R_2$ , is shown in Fig. 6(b). It reveals a weak dependence on  $R_2$ . This behaviour allows rather large fabrication tolerances without compromising the directionality too much.

Having studied even-symmetry modes in detail, let us now

briefly turn to the odd symmetry case. In a perfect disk without hole the odd and even symmetric modes are degenerate. The introduction of a hole only slightly lifts this degeneracy for low-radial order WGMs. Since, however, the ARC scenario is different for even and odd symmetry, the respective far-field pattern will differ. Hence, a light emitter couples easily to both WGMs which possibly leads to non-directed emission. This problem is resolved in the following cases: (i) In realistic microdisks, the double-degeneracy is lifted due to Rayleigh scattering from the disk surface [6]. (ii) For a single-photon source it is desired to place a single light emitter (e.g. a quantum dot) on an antinode of an optical mode in order to enhance light-matter interaction. In such a case, the emitter does not couple to the mode from the other symmetry class since it is placed on a node of that mode. (iii) It is possible to find pairs of ultra-high- $Q$  WGMs showing simultaneously highly-directed output, see inset in Fig. 4. In this particular case, the maxima of the far-field patterns are displaced from each other which is interesting for applications like all-optical switches and sensors.

Finally, the angular divergence of the output beam in vertical direction can be estimated to be  $2/\sqrt{m}$  as in the case of an ideal disk [28]. For our examples with  $m = 19, 34, 38$  follow angular divergences of  $26.3^\circ, 19.7^\circ, 18.6^\circ$ .

In summary, we presented a new general concept to achieve unidirectional light emission from high- $Q$  modes in microcavities utilizing resonance-enhanced dynamical tunneling. For a pierced microdisk, we showed unidirectional emission from modes with ultra-high  $Q > 10^8$ .

We would like to thank T. Harayama, S. Shinohara, S. Sunada, H. Lohmeyer, N. Baer, and F. Jahnke for discussions. J.W. acknowledges financial support by the Deutsche Forschungsgemeinschaft.

- 
- [1] K. J. Vahala, *Nature* **424**, 839 (2003).  
 [2] S. L. McCall, A. F. J. Levi, R. E. Slusher, S. J. Pearton, and R. A. Logan, *Appl. Phys. Lett.* **60**, 289 (1992).  
 [3] L. Collot, V. Lefevre-Seguin, M. Brune, J. Raimond, and S. Haroche, *Europhys. Lett.* **23**, 87 (1993).  
 [4] V. S. Ilchenko, M. L. Gorodetsky, X. S. Yao, and L. Maleki, *Opt. Lett.* **26**, 256 (2001).  
 [5] K. Srinivasan, M. Borselli, T. J. Johnson, P. Barclay, P. Painter, A. Stintz, and S. Krishna, *Appl. Phys. Lett.* **86**, 151106 (2005).  
 [6] M. Borselli, K. Srinivasan, P. E. Barclay, and P. Painter, *Appl. Phys. Lett.* **85**, 3693 (2004).  
 [7] H. Rigneault, J. Broudic, B. Gayral, and J. M. Gérard, *Opt. Lett.* **26**, 1595 (2001).  
 [8] A. F. J. Levi, R. E. Slusher, S. L. McCall, S. J. Pearton, and R. A. Logan, *Appl. Phys. Lett.* **62**, 561 (1993).  
 [9] J. U. Nöckel and A. D. Stone, *Nature* **385**, 45 (1997).  
 [10] M. S. Kurdoglyan, S.-Y. Lee, S. Rim, and C.-M. Kim, *Opt. Lett.* **29**, 2758 (2004).  
 [11] M. Kneissl, M. Teepe, N. Miyashita, N. M. Johnson, G. D. Chern, and R. K. Chang, *Appl. Phys. Lett.* **84**, 2485 (2004).  
 [12] D. Y. Chu, M. K. Chin, W. G. Bi, C. W. Tu, and S. Ho, *Appl. Phys. Lett.* **65**, 3167 (1994).  
 [13] V. M. Apalkov and M. E. Raikh, *Phys. Rev. B* **70**, 195317 (2004).  
 [14] S. Lacey, H. Wang, D. H. Foster, and J. U. Nöckel, *Phys. Rev. Lett.* **91**, 033902 (2003).  
 [15] M. J. Davis and E. J. Heller, *J. Chem. Phys.* **75**, 246 (1981).  
 [16] W. D. Heiss, *Phys. Rev. E* **61**, 929 (2000).  
 [17] M. Hentschel and K. Richter, *Phys. Rev. E* **66**, 056207 (2002).  
 [18] H. Schomerus, J. Wiersig, and M. Hentschel, *Phys. Rev. A* **70**, 012703 (2004).  
 [19] G. Hackenbroich and J. U. Nöckel, *Europhys. Lett.* **39**, 371 (1997).  
 [20] S. D. Frischat and E. Doron, *Phys. Rev. E* **57**, 1421 (1998).  
 [21] O. Bohigas, D. Boosé, R. Eglydio de Carvalho, and V. Marvulle, *Nucl. Phys. A* **560**, 197 (1993).  
 [22] A. Badolato, K. Hennessy, M. Ataïre, J. Dreiser, E. Hu, P. M. Petroff, and A. Imamoglu, *Science* **308**, 1158 (2005).  
 [23] S. A. Backes, J. R. A. Cleaver, A. P. Heberle, J. J. Baumberg, and K. Köler, *Appl. Phys. Lett.* **74**, 176 (1999).  
 [24] E. Peter, P. Senellart, D. Martrou, A. Lemaitre, J. Hours, J. M. Gérard, and J. Bloch, *Phys. Rev. Lett.* **95**, 067401 (2005).  
 [25] J. Wiersig, *J. Opt. A: Pure Appl. Opt.* **5**, 53 (2003).  
 [26] M. Hentschel, H. Schomerus, and R. Schubert, *Europhys. Lett.*

- 62**, 636 (2003).
- [27] A. I. Rahachou and I. V. Zozoulenko, *J. Appl. Phys.* **94**, 7929 (2003).
- [28] B. J. Li and P.-L. Liu, *IEEE J. Quantum Elect.* **33**, 1489 (1997).